

Role of structural relaxations, chemical substitutions and polarization fields on the potential line-up in [0001] wurtzite GaN/Al systems

S. Picozzi, G. Profeta and A. Continenza

Istituto Nazionale di Fisica della Materia (INFM)

Dipartimento di Fisica, Università degli Studi di L'Aquila, 67010 Coppito (L'Aquila), Italy

S. Massidda

Istituto Nazionale di Fisica della Materia (INFM)

Dipartimento di Scienze Fisiche

Università degli Studi di Cagliari, 09124 Cagliari, Italy

and

A. J. Freeman

Department of Physics and Astronomy and Materials Research Center

Northwestern University, Evanston, IL 60208 (U.S.A.)

Abstract

First-principles full-potential linearized augmented plane wave (FLAPW) calculations are performed to clarify the role of the interface geometry on piezoelectric fields and on potential line-ups at the [0001]-wurtzite and [111]-zincblende GaN/Al junctions. The electric fields (polarity and magnitude) are found to be strongly affected by atomic relaxations in the interface region. A procedure is tested to evaluate the Schottky barrier in the presence of electric fields and used to show that their effect is quite small (a few tenths of an eV). These calculations assess the rectifying behaviour of the GaN/Al

contact, giving very good agreement with experimental values for the barrier. Stimulated by the complexity of the problem, we disentangle chemical and structural effects on the relevant properties (such as the potential discontinuity and electric fields) by studying auxiliary unrelaxed nitride/metal systems. Focusing on simple electronegativity arguments, we outline the leading mechanisms that result in the final values of the electric fields and Schottky barriers in these ideal interfaces. Finally, the transitivity rule in the presence of two inequivalent junctions is proved to give reliable results.

I. INTRODUCTION

Wide-bandgap electronic devices are expected to play an important role in the next generation of high-power and high-temperature applications. In particular, extensive work has been carried out in recent years on many popular semiconductors of this type - GaN, AlN and SiC^{1,2}. It is clear, however, that many efforts, theoretical as well as experimental, are still needed to bring the emergent device technology to maturity. Within this context, the GaN/metal interface represents one of the most well-studied topics¹, since it is not yet clear which are the basic mechanisms leading to the observed behavior - ohmic vs rectifying - of the final barrier. A key property of the nitrides is the presence of large spontaneous and piezoelectric fields, which have to be considered whenever these compounds are used as basic constituents of technological devices³. Within the framework of *ab-initio* simulations, extensive work has been carried out for nitride/metal contacts, but the GaN structure explored so far has always been zincblende with [001] as the ordering direction⁴. In contrast, however, most of the experimental work in this field is focused on the hexagonal wurtzite structure as the stable phase of GaN.^{5,6}

In this work, we present results obtained from first-principles calculations using the all-electron full-potential linearized augmented plane wave (FLAPW)⁷ method for [0001] w-GaN/Al and [111] z-GaN/Al interfaces. These systems can be directly compared, since

[111]–ordered zincblende and [0001]–ordered wurtzite have exactly the same coordination up to the third nearest neighbor shell and the interface geometry (in terms of number and direction of bonds between different atomic species at the junction) is exactly the same.

II. COMPUTATIONAL DETAILS

The calculations were performed using one of the most accurate and highly precise first principles density–functional based methods, namely the all-electron FLAPW code⁷. The core levels are treated fully relativistically, whereas the valence electrons are calculated semi–relativistically, *i.e.* without spin-orbit coupling. The Ga 3*d* states were treated as valence electrons, in order to fully allow their characteristic hybridization with the N 1*s* states. The exchange–correlation potential is treated within the local density approximation using the Hedin–Lundqvist parametrization⁸. The FLAPW code allows calculation of total energy and atomic–forces, so that the structural optimization of the atomic positions is achieved by first principles. The muffin–tin spheres were chosen as $R_{MT}^{Ga} = 2.0$ a.u., $R_{MT}^{Al} = 2.0$ a.u. and $R_{MT}^N = 1.6$ a.u. and the expansion in spherical harmonics in these regions was performed up to $l \leq 8$; in the interstitial part, a cut–off for the wave functions $k_{max} = 4.0$ a.u.^{–1} was used. The Brillouin zone sampling was done according to the Monkhorst–Pack scheme⁹, using 10 **k** points in the irreducible part of the zone.

III. STRUCTURAL PROPERTIES AND ENERGETICS

The unit cell employed contains 6 layers of GaN (*i.e.* 7 N and 6 Ga atoms) and 6 layers of Al, for a total of 19 atoms per cell. Tests performed with varying cell dimensions have shown that this particular choice of number of layers for each material (*i.e.* semiconductor and metal) is sufficient to recover the proper bulk conditions away from the interface: this represents a major requirement when dealing with potential line–up problems with the supercell approach.

The equilibrium atomic-force and total-energy optimized w-GaN lattice constants are $a = 3.16 \text{ \AA}$ and $c/a = 1.624$, with an internal parameter $u = 0.377$. The agreement with the experimental values¹⁰ $a = 3.16$, $c/a = 1.62$ and $u = 0.377$ is excellent, as is usual for FLAPW structural results obtained for III-V semiconductors.

In the following, we will discuss in detail all the different structures studied, focusing on their differences and similarities.

A. Relaxed [0001] w-GaN/Al and [111] z-GaN/Al

As far as the structural configuration is concerned, we remark that optimization of atomic positions is very delicate in the GaN/Al system. In fact, as shown in the z-GaN[001]/Al case, the Schottky barrier is very sensitive to the interface geometry, namely the interplanar distances in proximity to the junction⁴. Due to the polarity of the interface in the systems of interest here, we may expect an even stronger effect of the structural configuration. In fact, in both N-terminated w-GaN[0001]/Al and z-GaN[111]/Al, the two interfaces present in the unit cell are inequivalent; as clearly shown in Fig. 1, the interface N is bonded with 3 Ga and 1 Al on one side (A-type with the “long” Al-N bond parallel to the growth axis) and with 3 Al and 1 Ga on the other side (B-type with the “short” Al-N bond parallel to the growth axis, leading to an interplanar distance which is ideally one third of the bond length)¹¹.

All the atomic positions were allowed to relax; the relevant interface bond lengths in the optimized geometries are reported in Table I. First of all, we note that the differences between the zincblende and wurtzite systems are negligible (less than 0.1 % of the bond lengths) and this confirms the similarity of the z-GaN[111]/Al and w-GaN[0001]/Al. The Ga-N distances can be compared with the w-GaN bulk bond length of 1.92 \AA and are found to deviate only by 1 % with respect to the equilibrium Ga-N bond length, showing that the relaxations in the semiconductor side are rather small. As expected, only the *interface* atoms in the semiconductor side deviate slightly from the bulk w-GaN distances; already in the

second layer, the first-nearest-neighbor bond lengths typical of bulk w-GaN are recovered (within 0.3 %). On the other hand, the Al atoms in the metallic layer deviate from the typical interplanar Al-Al distance for [111] ordered fcc-Al strained on [0001] w-GaN ($z_{Al-Al} = 2.046 \text{ \AA}$) by as much as 10 %. However, the positions of the Al atoms far from the junction are not expected to play a major role in the evaluation of the Schottky barrier heights (see discussion below). Moreover, we find some major differences in the relaxations at the two inequivalent interfaces, which are mainly related to the Al-N bond lengths. At the B interface, the “short” Al-N bond length ($d_{Al-N}^A = 1.93 \text{ \AA}$) is more or less unaltered with respect to the bulk GaN bond length (by $< 0.4 \%$), so that Al perfectly replaces the Ga cation in a bulk GaN. On the other hand, at the A interface the “long” Al-N bond length ($d_{Al-N}^B = 1.89 \text{ \AA}$) is smaller by 2.2 % than the bulk GaN bond length and much closer to the bulk w-AlN bond length¹⁰ ($d_{Al-N}^{w-bulk} = 1.87 \text{ \AA}$). Therefore, the tendency of Al and N atoms to get closer is higher (lower) when they are aligned (not-aligned) along the growth direction.

B. Model GaN/Al systems

In order to further investigate the *effect of the relaxations*, we also considered:

- An “ideal” (*i.e.* unstrained) system (denoted as w-GaN/Al^{id}) obtained starting from [0001] ordered bulk w-GaN, where the anions in the second half of the cell have been removed and the Ga cations substituted with Al. This gives rise to a semiconductor/metal interface between w-GaN and Al with all the Ga-N and Al-N distances equal to those in w-GaN, while the Al-Al distances match those between cations in w-GaN.
- A “partially relaxed” system (denoted as w-GaN/Al^{pr}) where all the interface and subinterface interplanar distances are relaxed to those in the fully relaxed system and the Al-Al distances in the metal side are forced to be equal. This system will be helpful to understand the effects of displacing Al atoms far from the junction in terms of stability, SBH and electric fields.

We focus first on the stability of the different systems. We show in Table II the total energies per atomic species of the systems referred to the most stable interface (*i.e.* w-GaN/Al^{rel}) taken as reference: these quantities represent the energy gain per atom with respect to the fully relaxed system. We observe that the effect of the relaxations in the interface region is quite high (about 50 meV/atom in going from w-GaN/Al^{id} to w-GaN/Al^{pr}), even if the deviations in terms of bulk bond lengths are less than 2 %. On the other hand, the total energy is very stable when the Al atoms in the bulk metal region are relaxed: less than 5 meV/atom. As expected, it is very important to accurately optimize the interface geometry, while changes of the atomic positions within the bulk metallic region are far less energetically expensive. Also, in agreement with previous results¹², we found that zincblende GaN is not favored compared to the wurtzite phase (but only by at most 10 meV/atom)¹³.

C. Additional model systems

- *Unrelaxed z-XN/Y*, ($X, Y = \text{Ga}, \text{Al}$)

In order to separate *chemical* and *structural* contributions to the SBH, we considered some unrelaxed [111] ordered (z-XN/Y)^{id} systems, where X,Y = Ga, Al. In these ideal systems, all the N-X (X = Ga, Al) bond lengths are equal, leading to more “symmetric” junctions (compared to the relaxed systems). Moreover, let us recall that the zincblende undistorted structure does not show any spontaneous polarization fields because of symmetry. Now, these model nitride/metal interfaces are not meant to simulate realistic systems; in fact, α -Ga being the Ga stable structure, the interface relaxations and coordinations in the XN/Ga junctions would be completely different from those considered here. Nevertheless, we will take these ideal systems as reference structures: indeed, in these junctions the atomic positions are frozen and set equal; only the chemical species occupying the atomic sites differ, thus allowing us to separate chemical from structural effects.

Insights into the chemical bonding at the nitride/metal systems can be gained by fo-

cusing on the adhesion energy E_{ad} of these unrelaxed systems. In order to estimate the gain in energy when depositing Al or Ga on a nitride surface, we calculate the difference between the adhesion energies¹⁴ in the $(\text{GaN}/\text{Ga})^{id}$ and $(\text{GaN}/\text{Al})^{id}$ junctions; $E_{ad}(\text{GaN}/\text{Al})^{id} - E_{ad}(\text{GaN}/\text{Ga})^{id} = 1.04$ eV and $E_{ad}(\text{AlN}/\text{Al})^{id} - E_{ad}(\text{AlN}/\text{Ga})^{id} = 1.06$ eV. The positive sign of these energy values indicates the larger energy gain that favours deposition of Al versus Ga on the N-terminated nitride surface; this is in agreement with the more ionic character of the Al-N bond compared to Ga-N. Moreover, the similarity of the two values confirms that the gain in adhesion energy is similar for the two nitride surfaces.

- *Unrelaxed $z\text{-XN}/\text{Y}/\text{X}$ and $z\text{-YN}/\text{X}/\text{Y}$ ($X, Y = \text{Ga}, \text{Al}$)*

Finally, with the only purpose to *investigate the role of a single metallic interlayer on the final line-up and electric fields*, we also focused on two systems, $(z\text{-AlN}/\text{Ga}^{int}/\text{Al})^{id}$ and $(z\text{-GaN}/\text{Al}^{int}/\text{Ga})^{id}$. These systems are obtained starting from the ideal $(z\text{-XN}/\text{X})^{id}$ interfaces and substituting the first X atom on the metallic side for the Y cation (*i.e.* we start from the $(z\text{-AlN}/\text{Al})^{id}$ systems and substitute the first Al layer with Ga, ending up with the $(z\text{-AlN}/\text{Ga}^{int}/\text{Al})^{id}$ system.)

IV. ELECTRONIC PROPERTIES

Let us investigate the two inequivalent interfaces (A and B in Fig.1) in terms of their density of states of the wurtzite based systems (the $z\text{-GaN}/\text{Al}$ is very similar and therefore not discussed). In Fig. 2, we show the density of states (PDOS) projected on the interface Ga, N and Al atomic sites in the relaxed $w\text{-GaN}/\text{Al}$ junction for the A-type (panels (a), (b) and (c), respectively) and for the B type interface (panels (d), (e) and (f)). Both Fig. 2 (a) and (d) show that the sub-interface Ga atoms in both A and B-type junctions have a PDOS very similar to that of the Ga atom in bulk $w\text{-GaN}$, except for the appreciable DOS due to the metal induced gap states (MIGS). On the other hand, the interface N atoms clearly differ in the A and B-type junctions; note, in particular, that the feature at -8 eV in

panel (b) , mainly due to cation s states, is shifted towards lower binding energies (about -7 eV in panel (e)). A more careful investigation shows that many of the features in the N PDOS of the A-type junction are common to bulk w-GaN (dashed line in panel (b)), while the N PDOS in the B-type interface is more similar to the one in bulk w-AlN (dashed line in panel (e)). Furthermore, the Al interface DOS is remarkably different in the two inequivalent junctions: in terms of the PDOS, this atom resembles the cation in bulk w-AlN in type B (dashed line in panel (f)), whereas it shows a free-electron-like behaviour, close to the one in bulk fcc-Al (dashed line in panel (c)) in the A-type interface.

The metallicity of the Al atom is confirmed by the higher DOS in the band-gap region (*i.e.* from about -2 eV to the Fermi level, E_F) of the Al in the A-type compared to that in the B-type junction. A simple rationale can be found by considering the geometry of the two inequivalent interfaces shown in Fig.1; in the A type the four N sp^3 orbitals point towards three Ga and one Al, whereas the situation is reversed (*i.e.* three Al and one Ga) in the B type junction. Thus, we can reasonably expect the N atom to be similar to bulk w-GaN (w-AlN) in the A (B) interface. Moreover, note that the higher DOS at E_F of the A-type Al atom (panel (c)) suggests a more effective screening than that at the B interface (panel (f)).

Finally, the bond length does not greatly affect the DOS: in fact, the PDOS (not shown) in the “frozen” reference structure (w-GaN/Al)^{*id*}, having all the AlN and GaN distances equal to those in bulk w-GaN, shows features that are very similar to the PDOS of the relaxed system (where every cation-N distance is different). Therefore, the electronic behaviour is dictated by the number and direction of bonds established between different atoms rather than by the distance between the atomic species participating in the bond.

V. ELECTRIC FIELDS

The inequivalency of the A and B interfaces, in terms of different geometries and bond lengths, gives rise to electric fields; in addition, in the wurtzite-based systems, we expect the

presence of intrinsic polarization fields, which vanish by symmetry in the zincblende-based junctions. In Fig. 3, we show the N 1s core level binding energies (in eV) in the wurtzite based systems for the ideal, partially and fully relaxed systems; the binding energies have been shifted arbitrarily so as to let the central core level coincide with the zero. The slope of the excellent linear fits through the 1s binding energies gives directly the electric fields, and their magnitudes (in V/nm) are reported in Table III for all the systems examined. The interface N atoms have been excluded from the fit, since, due to charge rearrangement in proximity to the junction, they are subject to additional local effects.

We expect that the polarization charge giving rise to the electric field is strongly affected by the interface geometry: in fact, the polarity of the field changes in going from ideal to relaxed systems and, in particular, the field is directed from the A to the B interface in the relaxed systems, whereas the situation is reversed in the ideal case.

The mechanisms giving rise to the electric field are very complicated: the interplay of boundary conditions, charge redistribution at the inequivalent interfaces and screening effects suggest that the value and even the polarity of the field cannot be determined within simple electrostatic or electronegativity arguments. In this context, *ab-initio* simulations are the only way to take into account microscopic details of charge rearrangement and boundary conditions, giving a correct description of the overall electrostatics. It can be argued that the almost negligible electric field present in the unrelaxed interface is due to the tendency of Al to screen the electric field: this is undoubtedly true for every good metal. However, the large total energy difference between the ideal and relaxed interfaces in Table II suggests that the electrostatic energy accumulated in the semiconductor side by the field is negligible by far compared to other total energy terms related to structural relaxations. Furthermore, the differences between the values of the electric fields in the zincblende and wurtzite systems are quite small so that the presence of intrinsic polarization fields is not playing a significant role in the final determination of the potential line-up (see below).

Our results for the electric fields in the ideal systems are shown in Fig. 4. The polarity of the field is the same in all the ideal systems (the electric field going from the B to the

A-type interface), but the magnitude shows large variations. First note that a naive picture for the (z-GaN/Al) interface (see Fig. 3) would suggest that more symmetric interfaces (*i.e.* with similar anion-cation bond lengths at the two interfaces) would exhibit smaller fields. However, as shown in Fig. 4, this is not the case. Consider, for example, the (z-GaN/Ga)^{id} ideal interface whose atomic positions and species are exactly equivalent to the (z-GaN/Al)^{id}, with Ga replacing Al in the metal side: here the electric field has the same order of magnitude as in the relaxed systems (see Fig. 3), but with reversed polarity. This confirms the complexity of the problem and of the interplay of strain and chemical effects. However, we can give a rationale for some of the observed behavior. For example, we note that in all the systems with Al (Ga) at the interface, the electric field is negligible (quite large); therefore, it seems that the Al atom favors charge rearrangement (whether it comes from GaN or AlN) in such a way as to screen the electric field much more efficiently than Ga. As for the comparison between the two different nitrides, we expect on the basis of electronegativity and ionicity arguments a larger interface bond charge in AlN than in GaN: this is confirmed by most of the results shown in Fig. 4.

In order to clarify the role of the interface metal layer, we plot in Fig. 5 the difference between the macroscopic planar average of the valence charge densities for the (z-GaN/Ga)^{id} and (z-GaN/Al^{int}/Ga)^{id} systems as a function of the growth direction. The only difference between these two systems is the metal atom bonded with N; however, the resulting electric fields are very different (see Fig. 4). This shows that the major role in establishing the final field is played by the interface metal atom rather than by the screening properties of the metal side of the junction. In other terms, the electric field, at fixed periodic boundary conditions, is determined by “interface” effects rather than by “bulk” properties of the constituents. Moreover, Fig. 5 demonstrates the different electronegativity between Al and Ga: more charge is localized on the interface N atom when it is bonded to Al than to Ga; also, the charge difference integral (dashed line in Fig. 5) shows that this effect is more pronounced in the A-type interface, where the metal-N bond is parallel to the growth axis. This is in agreement with what was pointed out for the relaxed (GaN/Al)^{rel} systems: due

to the particular interface geometry, the A-type interface favors charge transfer from Al to N with respect to the B-type junction.

Finally, we observe that the effect of the Ga d electrons on the electric fields is absolutely negligible; in fact, if we consider the (z-GaN/Ga)^{*id*} interface and treat the Ga d states as *i*) valence or as *ii*) core electrons, we obtain exactly the same resulting electric field.

VI. SCHOTTKY BARRIER HEIGHTS

Let us now discuss the most technologically important property, the Schottky barrier height and its relation to the piezoelectric fields. Usually, within all-electron methods the SBH is evaluated following a procedure based on core levels taken as reference energies¹⁵. The final SBH is therefore expressed as:

$$\Phi = \Delta b + \Delta E_b \quad (1)$$

where Δb is the difference between the 1s Ga and Al core levels far from the junction and is typically an interface contribution. ΔE_b , on the other hand, is a bulk contribution and is given by the difference between the binding energies of the same core levels with respect to the valence band maximum and E_F in the semiconductor and in the metal, respectively: $\Delta E_b = (E_{VBM}^{GaN} - E_{1s}^{Ga}) - (E_{Fermi}^{Al} - E_{1s}^{Al})$. It has been shown that this procedure is exactly equivalent to the one based on macroscopic average potentials, traditionally used in pseudopotential methods¹⁶.

Within this approach¹⁶, the bulk term is the difference between the valence band edge in the semiconductor and the Fermi level in the metal, each measured with respect to the average electrostatic potential of the corresponding crystal; the interface contribution is the electrostatic potential line-up across the junction. However, evaluation of the barrier height in the presence of electric fields is not so straightforward and deserves an appropriate discussion. In fact, whenever an electric field is present within the semiconductor side, the core level binding energies (or equivalently the electrostatic potential) depends on the z position of the atom, so that the usual procedure given by Eq. 1 becomes ill-defined.

We therefore considered a linear extrapolation of the core level binding energies (or of the macroscopic average of the electrostatic potential) and take the reference energies used in Eq. 1 as the intercepts of this line with the two interface planes (defined in the next paragraph). We then added the binding energy of the semiconductor side and obtained two different values, whose distance from E_F in the superlattice give directly the SBHs. In this way, we implicitly assume that E_F in the metal side coincides with the Fermi level of the superlattice. This procedure is exactly equivalent to that based on the PDOS on the different atomic sites, where the SBH is given by the difference of the valence band maximum on an inner semiconducting atom (where bulk conditions are recovered) and the Fermi level in the supercell; previous studies⁴ show that the results agree with those obtained from Eq.1 within 0.1-0.2 eV.

It is now necessary to define the two A and B-type interface planes. To this end, we observe in Fig.6, showing the planar macroscopic average of the valence charge density, that the two interface dipoles - giving rise to the potential lineup - are centered on the N atom in the B-type interface, and half-way between Al and N in the A-type interface. These planes are (arbitrarily) defined as the interface planes. We kept this choice for all our structures since the dipole locations did not change in the different systems. Moreover, we can give an estimate of the uncertainty related to this arbitrary choice, by considering interface planes that coincide with the extremes of the interface region, namely the interface Al and N atoms. This leads to an error of the order of a few hundredths of an eV (< 0.06 eV), so that our overall numerical uncertainty on the final SBH values adds up to 0.15 eV (including also errors in core level binding energies, macroscopic potential evaluations, and the accuracy of determining E_F).

Now, since the supercell approach employed introduces artificially two different interfaces (A and B in Fig.1) and therefore spurious boundary conditions, it is worthwhile exploring whether this unrealistic model is reliable for the SBH evaluation or if instead it gives an SBH dependent on the boundary conditions. To this end, we considered a larger w-GaN/Al system (consisting of 17 GaN layers with 9 N, 8 Ga and 6 Al), with exactly the same interface

configuration (*i.e.* the same interplanar distances of the relevant atomic sites in proximity to the junction) as those previously considered. As shown in Fig. 7, we find that the electric field is different (or, equivalently, the potential has a larger slope in the smaller system), but the SBH remains constant. This clearly shows that: (*i*) the conserved property of the system is the SBH; electric fields modify accordingly so as to adjust to boundary conditions, keeping constant the difference of the SBH at the two inequivalent interfaces and (*ii*) our procedure in estimating the potential line-up is correct.

Let us now discuss the estimated values of the SBH in the different systems, reported in Table IV. Quasi-particle effects and spin-orbit coupling have been neglected. First of all, note, within our procedure to estimate the SBH, that the difference between the two potential line-ups at the inequivalent interfaces ($\Delta\Phi^{A-B}$) is given by the electric field times the thickness of the semiconductor region; this implies that for an infinite thickness, the electric field would vanish so as to maintain $\Delta\Phi^{A-B}$ finite. This is consistent with the different charge readjustment occurring at each interface so that the Schottky barrier height associated with each isolated interface is a well defined quantity, not dependent on boundary conditions¹⁷.

Within the numerical error estimated above, we observe that all the values are in the range 1.5-2.0 eV. In particular, due to the electric fields, the A-type interface has a barrier which is generally higher than the one at the B interface in the relaxed system, while the situation is reversed in the ideal structures, consistent with the discussion in Sect. V. However, the difference is only about 0.2 eV since the structural relaxations involved are relatively small.

A comparison between the Schottky barriers found here and the barrier value in cubic [001] ordered z-GaN/Al (1.51 eV⁴) is not straightforward since the interface morphology is very different. Nevertheless, if we compare bond lengths and interface geometry we find stronger similarities with the B-type relaxed interface, whose SBH comes out to be very close to the one found in the [001] orientation.

As for the comparison with available experimental values, we note that photoemission

measurements performed on Al films deposited on clean 1x1 [0001] GaN surfaces give a SBH of about 2 eV, which is fully consistent with our *ab-initio* results. This confirms the strong rectifying character of the GaN/Al contact.

Finally, in order to disentangle the *structural* from the *chemical* contribution to the SBH, let us discuss the values for the ideal systems reported in Table V together with the corresponding electric fields. First of all, the SBH for the (GaN/Y)^{id} (Y = Ga, Al) interfaces are generally smaller (from 1.7 to 2.0 eV) than those for the (AlN/Y)^{id} (from 2.4 to 2.8 eV); the rectifying behavior of the contact is therefore stronger for the more ionic AlN than for GaN. On the other hand, if we keep the semiconductor region fixed and change the metallic side of the junction, we note slightly smaller modifications of the barrier (within 0.3 eV). Further, we find, for Al contacts, that the difference between the SBH at the two interfaces is smaller than in the Ga junctions: this is consistent with the smaller electric fields found in the Al case and with the more effective screening properties of Al discussed above.

Let us now come to the effect of the metallic intralayer on the final barrier. Any difference in SBH of the XN/X junctions with and without the intralayer has to be ascribed to the interface term Δb of the potential line-up, since the bulk term ΔE_b is the same. The overall effect is quite small (at most 0.2 eV) and confirms that the change of the metallic atom is not so important for the final SBH value, if we keep the interface geometry constant.

It is interesting to check the potential line-up transitivity rule¹⁶ for these ideal systems in the presence of the two inequivalent interfaces. In our case, each interface (of A or B-type) can be thought of being composed of different stacked systems:

$$(XN/Y)_A^{id} = (XN/X)_A^{id} + (X/YN)_B^{id} + (YN/Y)_A^{id}$$

$$(XN/Y)_B^{id} = (XN/X)_B^{id} + (X/YN)_A^{id} + (YN/Y)_B^{id}$$

The transitivity rule is therefore expressed as:

$$\Phi^A(XN/Y) = \Phi^A(XN/X) - \Phi^B(YN/X) + \Phi^A(YN/Y)$$

For example, in our case $\Phi^A(AlN/Ga) = 2.42$ eV and $\Phi^B(AlN/Ga) = 2.84$ eV. From the transitivity rule, we would get in the first case:

$$\Phi^A(AlN/Al) - \Phi^B(GaN/Al) + \Phi^A(GaN/Ga) = 2.47 - 1.80 + 1.67 = 2.34 \text{ eV,}$$

whereas in the second case:

$$\Phi^B(\text{AlN}/\text{Al}) - \Phi^A(\text{GaN}/\text{Al}) + \Phi^B(\text{GaN}/\text{Ga}) = 2.55 - 1.69 + 1.95 = 2.81 \text{ eV}.$$

The agreement with the calculated $\Phi^A(\text{AlN}/\text{Ga})$ and $\Phi^B(\text{AlN}/\text{Ga})$ values is excellent (within the numerical accuracy), so that the transitivity rule gives reliable results. Furthermore, this is an additional test of the method proposed to evaluate the SBHs.

VII. CONCLUSIONS

We have performed *ab-initio* FLAPW calculations for the GaN/Al interface, considering both [111] ordered zincblende and [0001] wurtzite based systems. Our calculations focused on the effects that structural modifications have on total energies, electric fields and SBH. We have shown that the structural optimization in the interface region is, as expected, very important; for example, relaxation of the interface Al positions can even reverse the polarity of the piezoelectric fields due to the inequivalency of the A and B-type interfaces. The final value of the electric field is the result of a complicated interplay between boundary conditions, charge rearrangement at the two junctions and screening effects and cannot be simply justified on the basis of electronegativity arguments or bond morphology at the interface.

On the other hand, the SBH at fixed geometry is independent of boundary conditions. However, we have identified some leading mechanisms (based on simple ionicity arguments) in establishing the final electric fields in the case of unrelaxed systems, due to different chemical species in the nitride or metallic side of the junctions. Our procedure to estimate the SBH in the presence of electric fields is found to give reliable results that were tested by increasing the unit cell dimensions. We have shown that the value of the SBH is not greatly affected by the presence of the piezoelectric fields of whatever polarity; this can only lead to changes in the SBH of a few tenths of an eV. Good agreement with available experimental data is also found. Finally, the transitivity rule was tested in the case of ideal systems for both A and B interface types and provided SBH values in excellent agreement with the

calculated values; they showed the consistency of our calculations.

ACKNOWLEDGEMENTS

We acknowledge useful discussions with Dr. F. Bernardini and Dr. P. Ruggerone. Work supported by the U.S. National Science Foundation (through the Materials Research Center at Northwestern University).

TABLES

TABLE I. Interface bond lengths for the relevant atomic species (in Å) in the fully relaxed systems.

	$(\text{w-GaN/Al})^{rel}$		$(\text{z-GaN/Al})^{rel}$	
	A	B	A	B
d_{GaN}	1.94	1.95	1.94	1.94
d_{AlN}	1.89	1.93	1.89	1.93

TABLE II. Difference between the total energy (in meV/atom) of the reference system $(\text{w-GaN}[0001]/\text{Al})^{rel}$ and that of the other interfaces, divided by the number of atoms. The estimated error is about 2 meV/atom.

$(\text{w-GaN/Al})^{rel}$	$(\text{z-GaN/Al})^{rel}$	$(\text{w-GaN/Al})^{pr}$	$(\text{w-GaN/Al})^{id}$	$(\text{z-GaN/Al})^{id}$
0	10	6	55	59

TABLE III. Electric fields in mV/Å. The positive sign is relative to the core levels being deeper in going from the B to A interface. The estimated error is about 0.5 mV/Å.

$(\text{w-GaN/Al})^{rel}$	$(\text{z-GaN/Al})^{rel}$	$(\text{w-GaN/Al})^{pr}$	$(\text{w-GaN/Al})^{id}$	$(\text{z-GaN/Al})^{id}$
23	14	31	-5	-7

TABLE IV. Schottky barrier heights (in eV) at the two inequivalent A and B type interfaces.

The estimated error is about 0.15 eV.

	$(\text{w-GaN/Al})^{rel}$	$(\text{z-GaN/Al})^{rel}$	$(\text{w-GaN/Al})^{pr}$	$(\text{w-GaN/Al})^{id}$	$(\text{z-GaN/Al})^{id}$
Φ^A	2.07	1.98	1.99	1.84	1.69
Φ^B	1.69	1.76	1.48	1.93	1.80

TABLE V. Electric fields (in mV/Angstrom) and Schottky barrier heights (in eV) at the two inequivalent A and B type interfaces for the unrelaxed systems.

	E	Φ^A	Φ^B
$(\text{z-GaN/Al})^{id}$	-7	1.69	1.80
$(\text{z-GaN/Ga})^{id}$	-17	1.67	1.95
$(\text{z-GaN/Al}^{int}/\text{Ga})^{id}$	-5	1.91	2.00
$(\text{z-AlN/Ga})^{id}$	-25	2.42	2.84
$(\text{z-AlN/Al})^{id}$	-5	2.47	2.55
$(\text{z-AlN/Ga}^{int}/\text{Al})^{id}$	-18	2.40	2.70

FIGURES

FIG. 1. Interface geometry at the inequivalent A and B junctions.

FIG. 2. Projected density of states (states/eV-atom) on the interface Ga (panels (a) and (d)), N (panels (b) and (e)) and Al atoms (panels (c) and (f)) in the A and B-type (w-GaN/Al)^{rel} interface, respectively.

FIG. 3. N 1s core levels (in eV) vs coordinate along the growth axis (in Å) for the ideal (filled circles), partially relaxed (diamonds) and relaxed (grey squares) GaN/Al interfaces. Core levels have been arbitrarily shifted so that the central core level in each of the three systems coincides with the zero of the energy scale.

FIG. 4. Linear fit of the N 1s core levels (in eV) vs growth axis (in Å) in the nitride bulk region. The slope gives the electric field.

FIG. 5. Difference between the macroscopic average of the valence charge densities in the (z-GaN/Ga)^{id} and (z-GaN/Al^{int}/Ga)^{id} interfaces along the growth axis (solid line). Also shown is its integral (dashed line).

FIG. 6. Macroscopic average of the valence charge density in the (w-GaN/Al)^{rel} interface along the growth axis.

FIG. 7. Macroscopic average of the electrostatic potential (in eV) in the semiconductor side of the (w-GaN/Al)^{rel} interface along the growth direction: comparison between the two cells containing 13 (solid) and 17 (dashed) GaN layers.

REFERENCES

- ¹ See for example P. Kung and M. Razeghi, *Opto-electronics Review* **8**, 201 (2000) or *Solid State Electronics* **42**, 677 (1998).
- ² P. Ferrara, N. Binggeli and A. Baldereschi, *Phys. Rev. B* **55**, R7418 (1997).
- ³ F. Bernardini and V. Fiorentini, *Appl. Surf. Sci* **166**, 23 (2000); A. Di Carlo, F. Della Sala, P. Lugli, V. Fiorentini and F. Bernardini, *Appl. Phys. Lett.* **76**, 3950 (2000).
- ⁴ S. Picozzi, A. Continenza, G. Satta, S. Massidda and A. J. Freeman, *Phys. Rev. B* **61**, 16736 (2000); S. Picozzi, A. Continenza, S. Massidda, N. Newman and A. J. Freeman, *Phys. Rev. B* **58**, 7906 (1998).
- ⁵ U. Karrer, O. Ambacher and M. Stutzmann, *Appl. Phys. Lett.* **77**, 2012 (2000).
- ⁶ V. M. Bermudez, T. M. Jung, K. Doverspike and A. E. Wickenden, *J. Appl. Phys.* **79**, 110 (1996).
- ⁷ E. Wimmer, H. Krakauer, M. Weinert, and A. J. Freeman, *Phys. Rev. B* **24**, 864 (1981); H. J. F. Jansen and A. J. Freeman, *ibid.* **30**, 561 (1984) and references therein.
- ⁸ L. Hedin and B. I. Lundqvist, *J. Phys. C* **4**, 2062 (1971).
- ⁹ H. J. Monkhorst and J. D. Pack, *Phys. Rev. B* **13**, 5188 (1976).
- ¹⁰ *Numerical Data and Functional Relationships in Science and Technology*, edited by K. H. Hellwege, Landolt Börnstein Tables, Group III, Vol. 17a (Springer, New York, 1982).
- ¹¹ Note that this doubles the computational load required to optimize the several structural degrees of freedom (*i.e.* the atomic positions in the interface region) with respect to the [001] z-GaN/Al case, where the two junctions are exactly equivalent.
- ¹² C. Y. Yeh, S. H. Wei and A. Zunger, *Phys. Rev. B* **50**, 2715 (1994).
- ¹³ This is consistent with the observed possibility of epitaxially growing cubic instead of

hexagonal GaN under specific conditions.

¹⁴ As usual, the adhesion energy is defined following R. Stadler, D. Vogtenhuber and R. Podloucky, Phys. Rev. B **60**, 17112 (1999) and references therein.

¹⁵ S. Massidda, B. I. Min and A. J. Freeman, Phys. Rev. B **35**, 9871 (1987).

¹⁶ S. Baroni, R. Resta, A. Baldereschi and M. Peressi, in *Spectroscopy of Semiconductor Microstructures*, edited by G. Fasol, A. Fasolino and P. Lugli (Plenum, New York, 1989), p. 251.

¹⁷ A. Ruini, R. Resta and S. Baroni, Phys. Rev. B **57**, 5742 (1998).

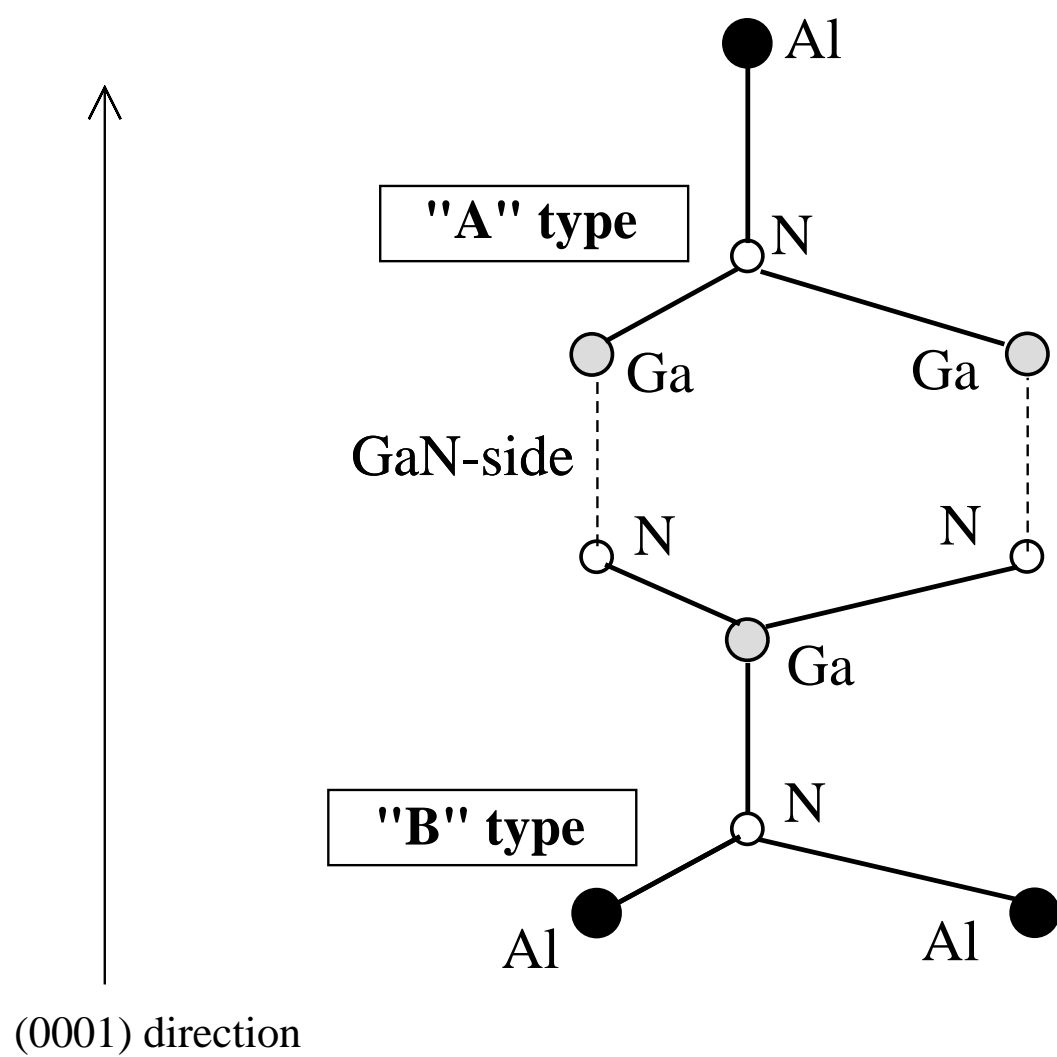
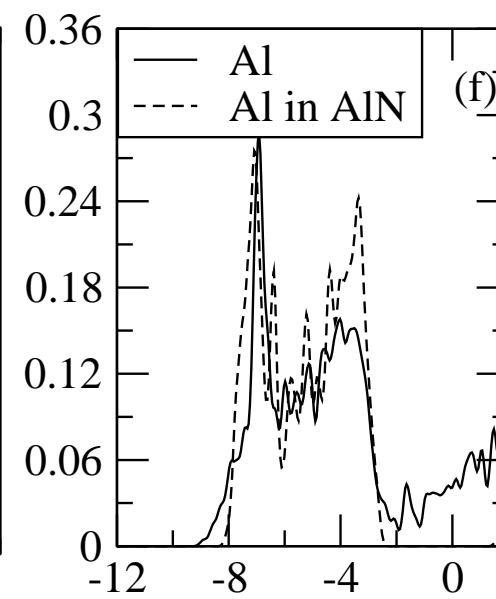
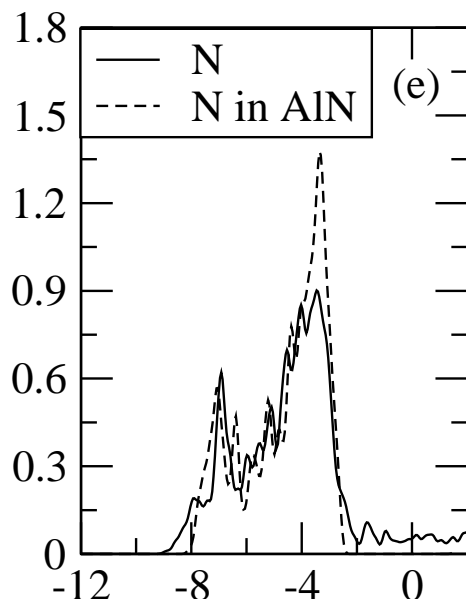
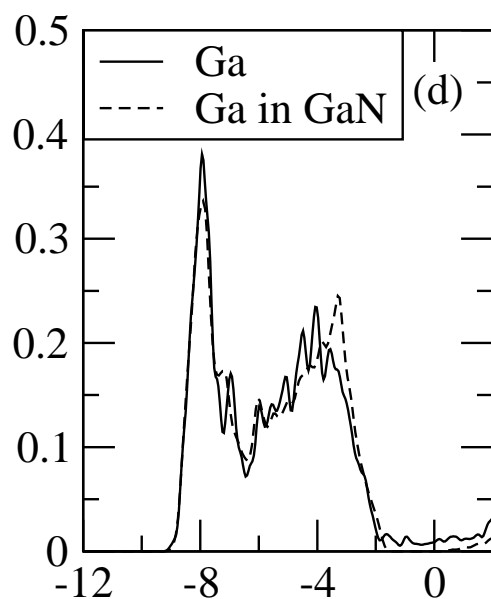
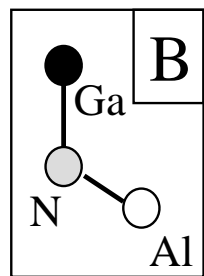
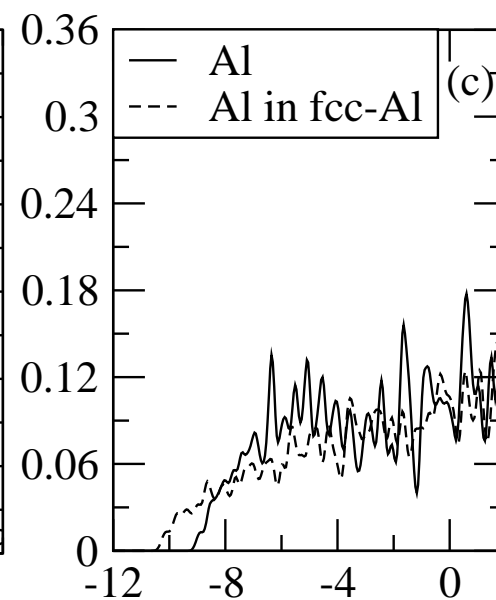
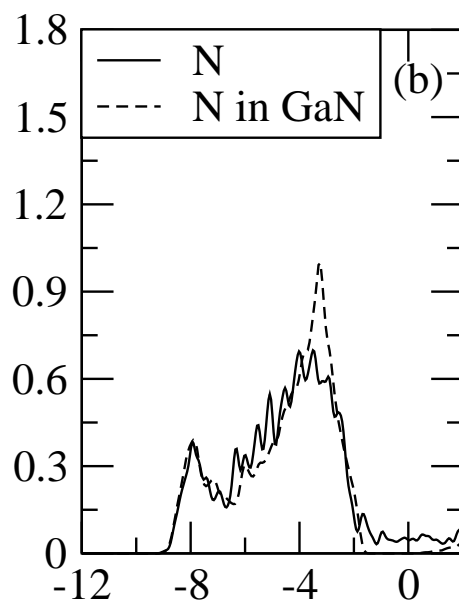
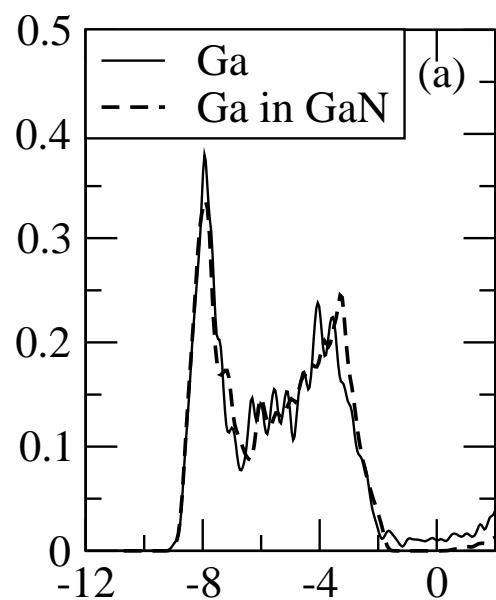
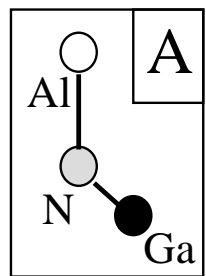


Fig. 1 - Picozzi et al.



E (eV)

Fig.2 . Picozzi et al.

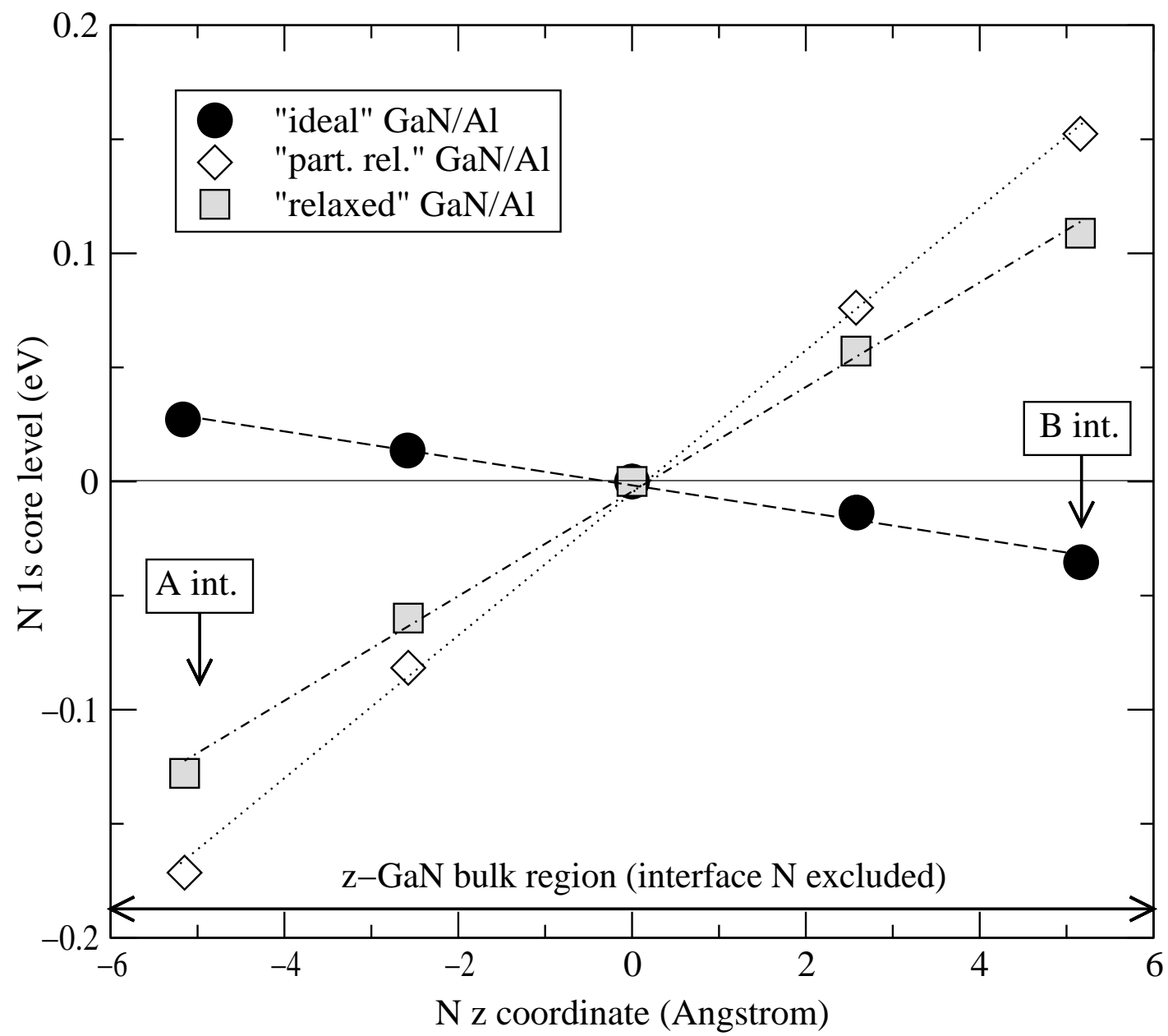


Fig. 3 – Picozzi et al.

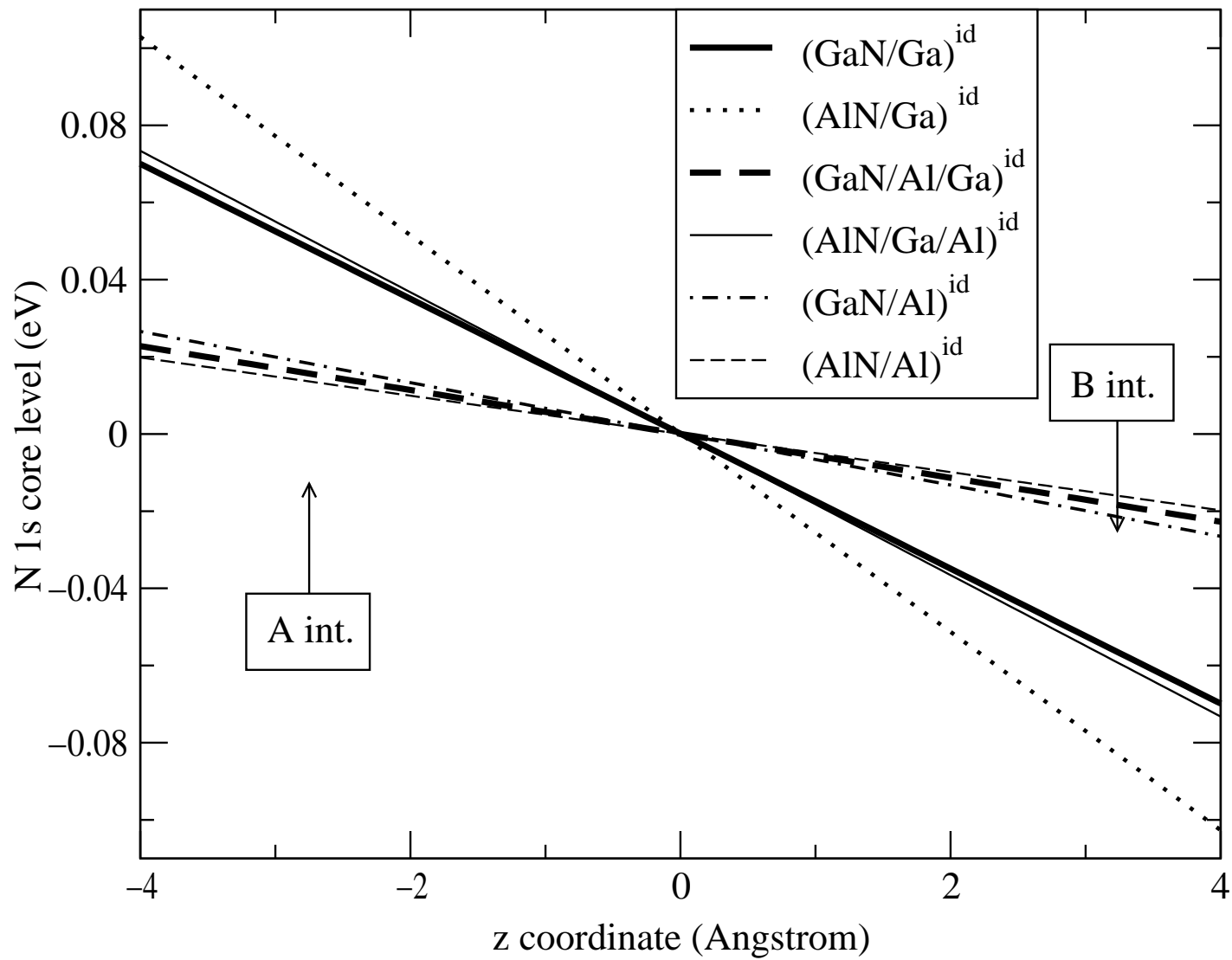


Fig. 4 – Picozzi et al.

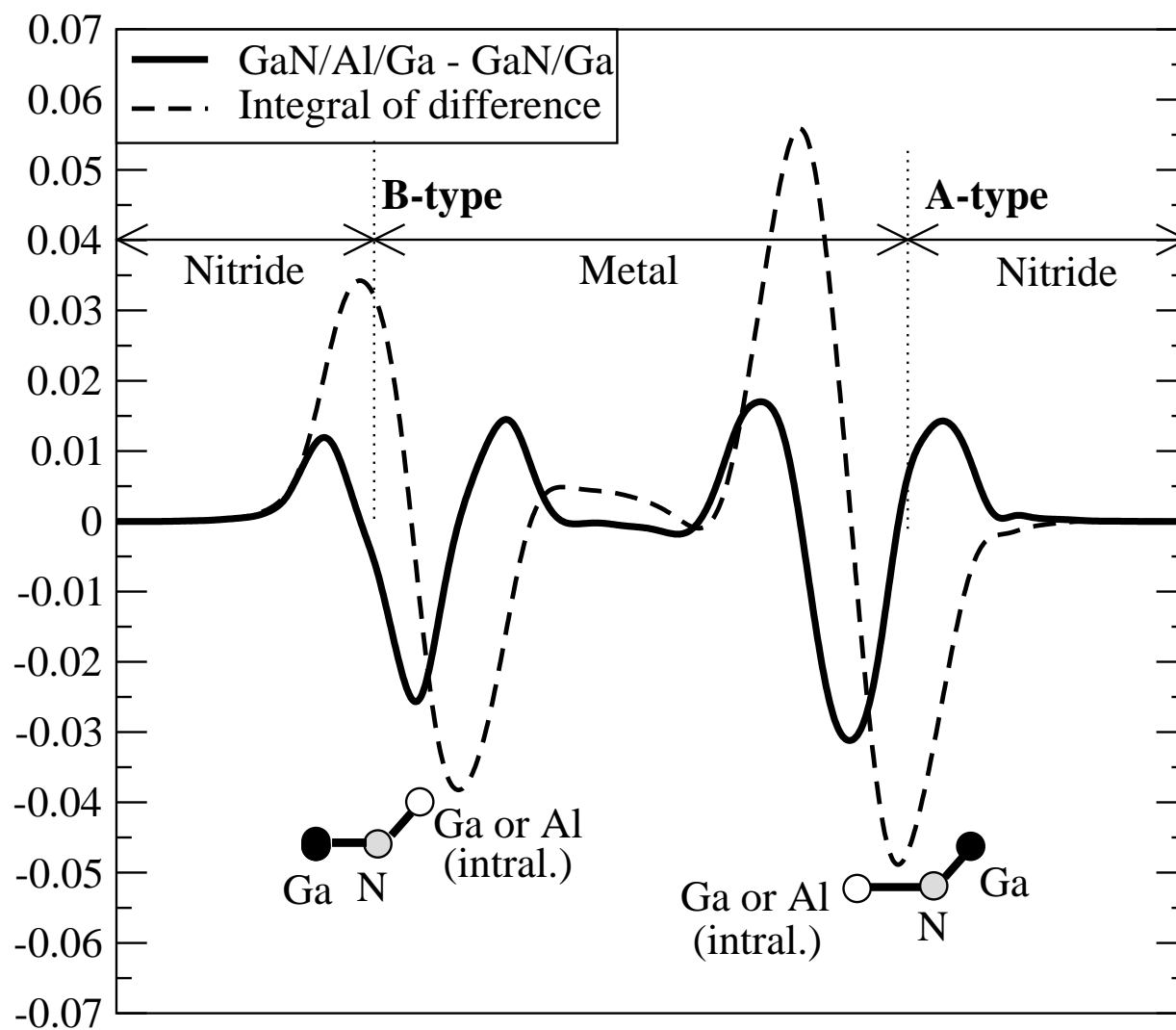


Fig. 5 - Picozzi et al.

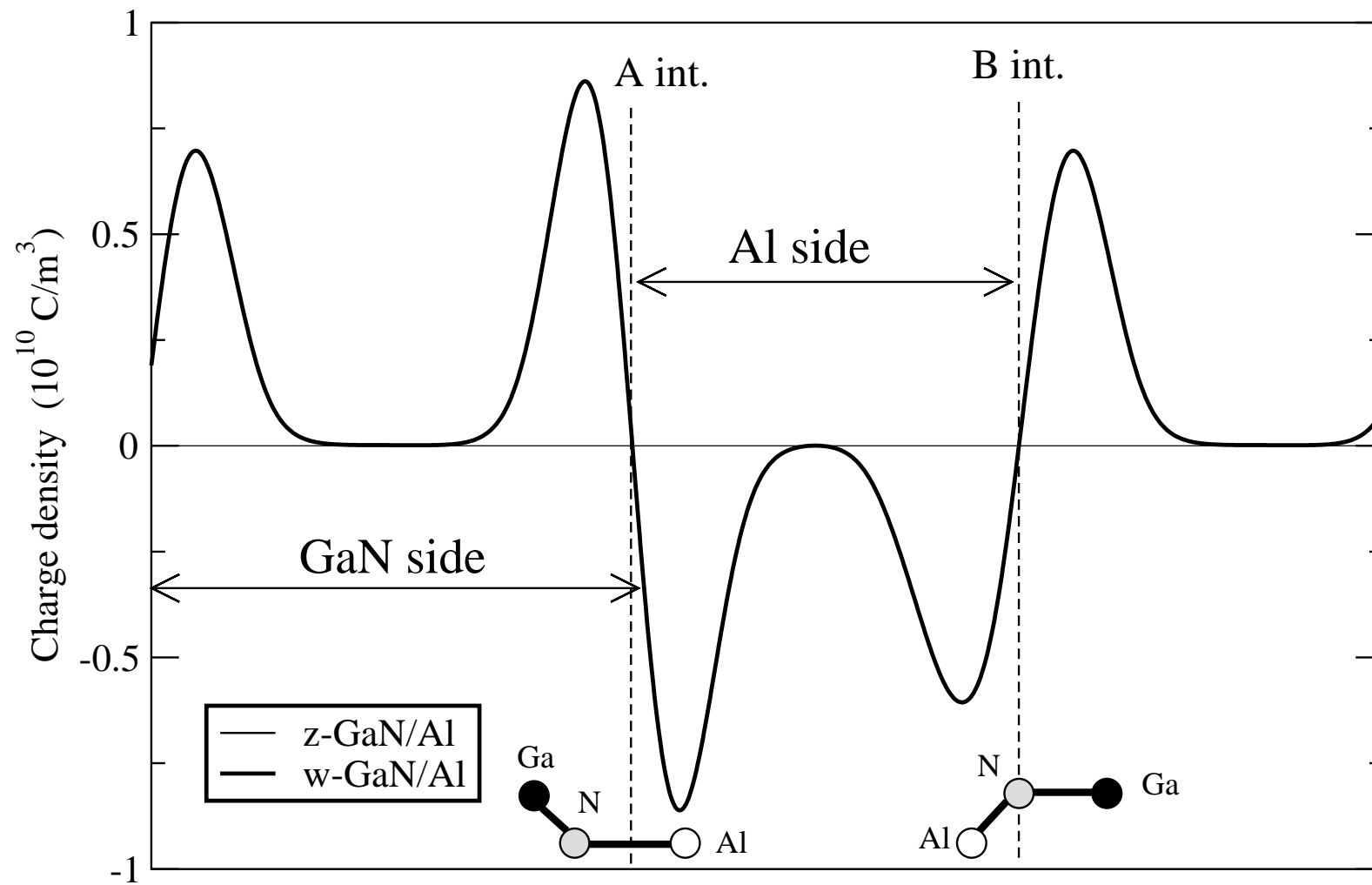


Fig. 6 - Picozzi et al.

Fig. 7 - Picozzi et al.

